Solid State Communications 250 (2017) 108–111

Contents lists available at ScienceDirect

Solid State Communications

journal homepage: www.elsevier.com/locate/ssc

Communication

Electronic structures and half-metallicity of carbon doped bulk and surface CdS: The modified Becke-Johnson potential calculation

X.N. Huang, S.W. Fan*, L.Q. Pan

Department of Physics, China Three Gorges University, Yichang 443002, China

ARTICLE INFO

Keywords:
C. Electronic structures
B. Modified Becke-Johnson potential
D. Ferromagnetism

ABSTRACT

The electronic structures and ferromagnetism for bulk and surface CdS with C_S defects are investigated by the full potential linearized augmented plane wave method together with the modified Becke-Johnson potential. Calculations show bulk and surface CdS with C_S defects are half-metallic ferromagnet. Each C_S defect could produce the total magnetic moment of 2.00 μ_B. Electronic structures indicate the stable ferromagnetism could be attributed to the p-d exchange-like p-p coupling mechanism. Sulfur vacancies would give rise to the magnetism vanishing. For the nonpolar $(10\bar{1}0)$ surfaces, the C_S defects prefer to occupy the surface layer sites.

1. Introduction

Due to the rich physics and potential applications in spintronics [1,2], diluted magnetic semiconductors (DMSs) with room-temperature ferromagnetism have attracted considerable attentions. During past decades, the room temperature ferromagnetism has been found in transition metal elements (TMs)-doped DMSs, such as, TMs-doped ZnO [3], GaN [4], In_2O_3[5] and TiO_2[6], etc. However, the ferromagnetism for TMs-doped DMSs usually suffers from the TMs aggregations or secondary phase, and few convincing evidences could verify the ferromagnetism of TMs-doped DMSs is intrinsic [7]. Recently, the room temperature ferromagnetism for C-doped ZnO [8,9], In_2O_3[10] and BN [11], as well as N-doped ZnO [12] have been reported. Moreover, several theoretical works have also predicted the ferromagnetism could be obtained in C-doped ZnS [13,14], CdS [15,16], AlN [17] and TiO_2[18], as well as the N-doped ZnO [19], TiO_2[20] and In_2O_3[21]. These researches indicate the C and N could be selected as dopants to fabricate DMSs. Due to the C and N have no *d* or *f* electrons, the C or N-doped DMSs are described as d^0-type DMSs, in which the secondary phases induced by dopants could not provide magnetism.

Cadmium sulfide (CdS), as one of the group II-VI semiconductor, has obtained wide recognition for its outstanding optical-electronic properties [22]. Due to its direct wide band gap (2.58 eV) [23], CdS is of considerable importance in optoelectronic applications and also used as an n-type window material in thin-film solar cell devices [24–26]. Utilizing the generalized gradient approximation (GGA) [27], the electronic structures and ferromagnetism for C-doped CdS have been investigated [15,16]. In addition, the formation energy for CdS within single C_S defect is only 1.20 eV [15]. However, few works concern the electronic structures and magnetism for C-doped surface CdS. Furthermore, the GGA and local density approximation (LDA) calculations always severely underestimate the energy gap of semiconductors, and therefore the position of defect levels suffers from large uncertainties [28]. For the d^0-type DMSs, underestimating energy gap usually results in the 2p defect states tending to come out too extended. Therefore, the ferromagnetism obtained by traditional GGA and LDA calculations might be optimistic and unreliable [29]. To obtain the accurate band gap, LDA (GGA) plus U [30] and self-interaction correction [31] have been proposed. However, LDA (GGA) plus U [32] and self-interaction correction [33] schemes emphasize Coulomb correlation in the 2p hole states which strongly localizes the 2p hole states (and the associated magnetic moments) and then impedes ferromagnetism (combining with the local Jahn-Teller distortion) [29]. To obtain the relative real properties and electronic structures for C-doped bulk and surface CdS, modified Becke-Johnson potential (mBJ) [34] is selected as the exchange correlation potential, which is mainly due to the mBJ potential has been successfully applied to obtain the accurate energy gaps for the semiconductors, insulators and oxides [34–37], half-metallic systems [38–41], as well as d^0-type DMSs [42–45]. Our investigations show that C_S defects could induce both bulk and surface CdS to be half-metallic ferromagnet. Single C_S defect could produce the total magnetic moment 2.00 μ_B. Sulfur vacancies would force the magnetism vanishing. For C-doped $(10\bar{1}0)$ surfaces, the C_S defects tend to occupy the surface layer sites and the ferromagnetic coupling still exists among C dopants.

* Corresponding author.
E-mail address: fansw1129@126.com (S.W. Fan).

http://dx.doi.org/10.1016/j.ssc.2016.11.024
Received 10 October 2016; Received in revised form 18 November 2016; Accepted 28 November 2016
Available online 29 November 2016

2. Computational details

Electronic structures and magnetism are calculated by using the full potential linearized augmented plane wave method (FP_LAPW), as implemented in WIEN2K package [46]. The GGA (PBE) [27] and mBJ [34] are selected as the exchange correlation potential. In present work, the muffin-tin sphere radii R_{mt} of Cd, S and C are set to 2.37, 2.17 and 1.80 Bohr, respectively. The $R_{mt}K_{max}$ is set to 7.80. The Monkhorst-Pack k-point meshes of 3×3×2 are employed to sample the irreducible Brillouin-zone for 3×3×2 supercells. The angular momentum expansion is up to l_{max}=12 in the muffin-tins. Self-consistency is achieved when the energy difference between succeeding iterations is less than 10^{-4}Ry. During structural optimization, the pseudopotentials plane wave method performed by CASTEP package [47] is utilized to optimize the lattice parameters and atoms' positions simultaneously. The cutoff energy is set to 280.0 eV. The 3×3×3 k-point grids are adopted for the Brillouin-zone integrations for 3×3×2 supercells. Convergence of structural optimizations are realized when the energy difference between the succeeding iterations is less than 10^{-5} eV/atom.

3. Results and discussions

Based on the experimental wurtzite lattice parameters [48], the 3×3×2 supercells, in which a sulfur is substituted by carbon to form the C_S doped configuration, are built (Fig. 1, site a). Structural relaxations, performed by GGA, show that the C-Cd bonds length along the hexagonal c-axis (other three equivalent) directions decrease to 2.241 (2.272) Å, such bonds are slightly shorter than that of the corresponding ideal S-Cd bonds 2.575 (2.587) Å, which is consistent with Pan et al.'s results [15]. The slightly suppression for the C-Cd bonds could be attributed to the radius of C (70 pm) is less than that of S (100 pm) [49].

Spin and non-spin polarized calculations, performed by GGA, show that CdS containing single C_S defect favors the spin polarized state with energy difference of 190.40 meV. Based on the relaxed structures, the

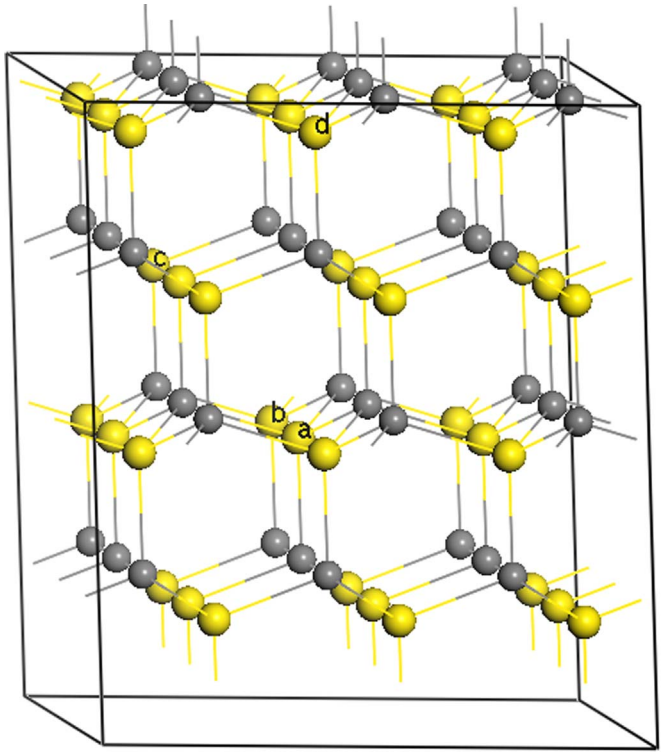

Fig. 1. (Color online) The positions of sulfur substituted by carbon are denoted by a-d, respectively. Yellow (gray) balls indicate sulfur (cadmium), respectively.

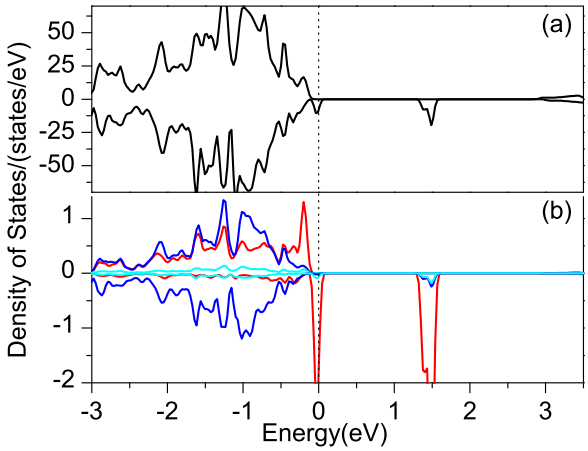

Fig. 2. (Color online) Total density of states for 3×3×2 supercell with single C_S defect, calculated by mBJ, is shown in (a). Partial density of states for C-2p, S-3p and Cd-4d, represented by the red, blue and cyan lines, are illustrated in (b). The vertical dashed line represents the Fermi level.

density of states (DOSs), calculated by mBJ potential, are shown in the Fig. 2. Total DOSs (Fig. 2(a)) shows an obvious spin-splitting between the majority and minority -spin states near the Fermi level, which indicates that C_S defect could induce CdS to be magnetic system. The DOSs show the majority-spin channel displays semiconductor behavior with the energy gap (2.60 eV), which is much larger than Pan *et al.*'s GGA result (1.11 eV) [15]. While the minority-spin channel crosses the Fermi level and shows metallic characters. The DOSs indicates that C_S defect could induce the CdS to be half-metallic ferromagnet. The partial DOSs (Fig. 2(b)) for the C-2p, and its neighboring Cd-4d as well as the next neighboring S-3p show the impurity bands near Fermi level are mainly constituted by C-2p states, which is due to the smaller radium of C than S. Smaller radium of C would result in the less interactions between dopants and host atoms, and force the bonding (antibonding) states interacting with the valence band (conduction band). Hence, the impurity states could not be pulled up (pushed down) to the conduction band (valence band) and located in the band gap. Compared to the GGA' results [15], the energy gap increasing induces the C-2p states in the minority-spin channel to move to high energy region and form the larger spin-splitting. The total magnetic moment for CdS with single C_S defect still keeps as 2.00 μ_B. The magnetic moment for carbon dopant reduce from the 1.12 μ_B[15] to 0.96 μ_B, which further confirms the underestimating energy gap would result in the overly optimistic prediction the magnetism for the d^0elements doped semiconductors.

To further study the stability of the ferromagnetic phase with respect to the antiferromagnetic phase, several pairs doped configurations are constructed (Fig. 1, sites a-d). Pairs (a, b), (a, c) and (a, d) correspond to the first, second and fifth neighboring C-C atoms, respectively. Based on the fully relaxed structures, spin polarized calculations for the parallel and anti-parallel spin arrangement on C dopants (corresponding to ferromagnetic and antiferromagnetic phase) are performed by mBJ potential. The corresponding energy differences ($\Delta E_{FM}=E_{AFM}-E_{FM}$) for the above built pair doped configurations are 27.20, 137.30 and 62.46 meV, implying ferromagnetic coupling interaction between double C dopants could extend to the fifth neighboring (7.984 Å). This tendency for energy difference ($\Delta E_{FM}=E_{AFM}-E_{FM}$) is consistent with Pan *et al.*'s results [15]. Furthermore, these energy differences are larger than those of GGA's results [15], which is mainly due to the mBJ potential could produce the large energy gap as well as the larger spin splitting.

Due to the quantum-mechanical level repulsion, the spin splitting emerges between majority and minority -spin channels and the C-2p states split into more stable three-fold t_2 states. The symmetry and wave function of impurity p-like t_2 states are similar to those of anion p states, thus giving rise to a strong p-p coupling interaction between C-

2p and S-3p orbitals. The spin polarized holes would be introduced into valence bands with C injecting into CdS host. The strong p-p interaction causes stronger coupling between the spin orientations of C dopants and its neighboring carriers. Consequently, the spin directions of carriers near each impurity atom tend to align parallel to the impurity moment. If the concentration of spin polarized carriers is sufficiently high, it is possible to mediate the spin alignment of impurities and thus facilitate an indirect long-range ferromagnetic coupling between C dopants. Hence, the p-d exchange-like p-p coupling interaction between C-2p and S-3p states [19] could be used to explain the stable ferromagnetism for C-doped CdS.

To confirm the attractive or repulsive interactions between C dopants, chemical pair interactions (V_{ij}) are calculated by the following formula [50],

$$V_{ij} = E(Cd_{36}S_{36}) + E(Cd_{36}S_{34}C_2) - 2E(Cd_{36}S_{35}C_1). \quad (1)$$

where $E(Cd_{36}S_{36})$, $E(Cd_{36}S_{35}C_1)$ and $E(Cd_{36}S_{34}C_2)$ are the energies for the supercells with zero, single and double C_S defects, respectively. Utilizing GGA, the chemical pair interactions are calculated. The chemical pair interactions for (a, b), (a, c) and (a, d) pairs doped configurations are −2.37, −2.18 and −2.26 eV, respectively. The negative chemical pair interactions indicate that the attractive interactions exist among C dopants [50], implying that the C_S defects in CdS hosts tend to form the spinodal nano-decomposition phase. Hence, it is necessary to select the fabricated method to restrict the C_S clustering formations during the samples fabricated.

To enhance the solubility of C_S defects, the anion poor condition should be kept during the samples fabricated [51]. Anion poor condition would result in the anion vacancies emerging. To study the effects of sulfur vacancy on magnetism, several sulfur vacancy sites are constructed in the 3×3×2 supercell with single C_S defect. The geometry optimization, performed by GGA, shows sulfur vacancy favors emerging near the C dopant. Spin polarized calculations indicate the total magnetic moment decreases to zero and the magnetic moment of C is reduced from 0.96 μ_B to 0.002 μ_B, which suggests the sulfur vacancy would force C-doped CdS to be nonmagnetic system. The spin polarized total DOSs (Fig. 3) shows the sulfur vacancy would induce C-doped CdS system to be paramagnetic metal. Therefore, sulfur vacancies should be restrained during the samples fabricated.

For practical applications, DMSs usually present in the form of films. Hence, it is significantly to investigate the magnetism for C-doped CdS surfaces. In present work, the $(10\bar{1}0)$ surfaces are modeled as 2×2 ten-layer (Fig. 4). To make the surfaces not couple with each other, each slab is separated from the other by 10 Å vacuum regions normal to the surfaces. Structural relaxations are performed by GGA for the top eight atomic layers in every slab. Four doped configurations, in which double S atoms replaced by C dopants at positions (a, b), (c, d), (e, f) and (f, g) are built (Fig. 4). After geometry optimizations, the

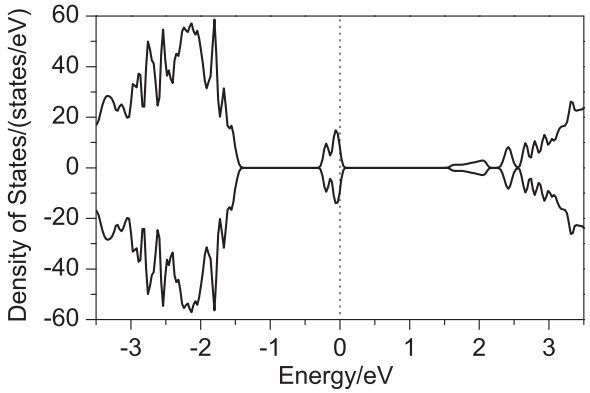

Fig. 3. Spin polarized total density of states for single C-doped 3×3×2 CdS supercell with sulfur vacancy, calculated by mBJ, is shown. The vertical dashed line represents the Fermi level.

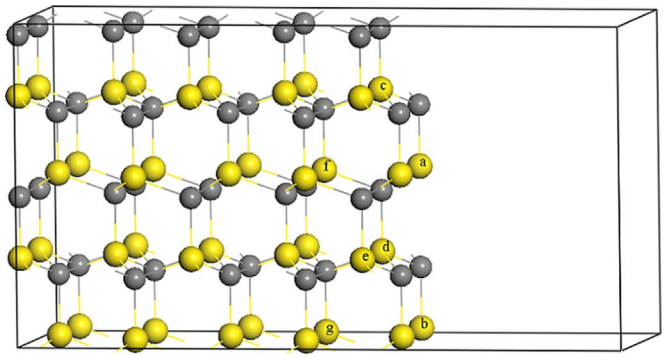

Fig. 4. (Color online) The ten-layer slab is used in the calculation. Yellow (gray) balls indicate sulfur (cadmium) atoms. The positions of sulfur substituted by carbon are denoted by a-g, respectively.

relative energies for the four doped configurations show C dopants favor to occupy the surface layer sites. Meanwhile, for the stable (a, b) doped configuration, C and Cd in the surface layer move 0.55 Å and 0.65 Å to subsurface layer as well as S in the same layer move slightly towards the vacuum layer by 0.10 Å. Spin polarized calculations, performed by mBJ potential, show the above built doped configurations all favor the ferromagnetic phase, and the energy differences (ΔE_{FM}=E_{AFM}-E_{FM}) for (a, b), (c, d), (e, f) and (f, g) doped configurations are 204.00, 613.21, 44.88 and 68.54 meV, respectively. Band structures for the stable (a, b) doped configuration (Fig. 5) show C-doped CdS $(10\bar{1}0)$ surfaces still maintain half-metallic ferromagnetism. The corresponding half-metallic gap is 0.31 eV, which is much larger than that of the bulk case (0.10 eV).

4. Conclusions

Utilizing the first-principles calculations, the magnetism and electronic structures for bulk and surface CdS with C_S defects are investigated. Our calculations show, as the band gap increases to the experimental value, the C_S defects could induce CdS to be a half-metallic ferromagnet, and each C_S defect could produce the total magnetic moment of 2.00 μ_B. The electronic structures indicate the ferromagnetism could be explained by the p-d exchange-like p-p coupling mechanism. Sulfur vacancies would force CdS with C_S defects losing the ferromagnetism. For C-doped CdS nonpolar $(10\bar{1}0)$ surfaces, carbon dopants have a tendency to occupy the surface layer sites and still keep the half-metallic ferromagnetic behavior. Our investigations indicate the CdS with the C_S defects would be promising materials to realize the spin polarization current injection. These findings suggest

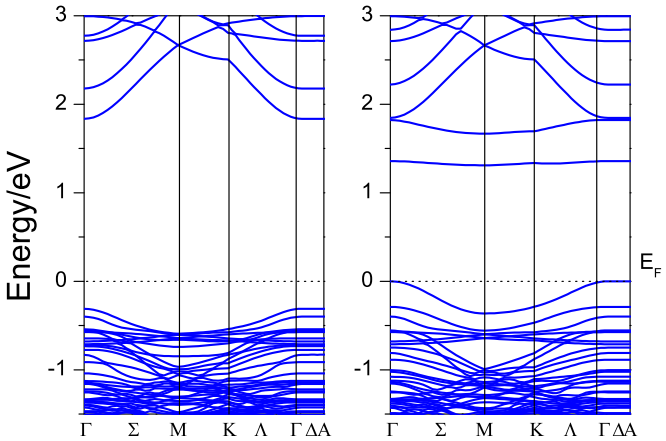

Fig. 5. Band structures for C-doped CdS $(10\bar{1}0)$ surface, calculated by mBJ, are shown. The left (right) column indicates the majority (minority) spin channel, respectively. The horizontal dashed line represents the Fermi level.

experimentally viable ways for controlling the magnetism in CdS hosts.

Acknowledgement

This work is supported by National Natural Science Foundation of China (Grant nos. 11174179 and 51371105). We also thank the National Supercomputing Centre in Shenzhen for providing the computational resources and Materials Studio.

References

[1] H. Ohno, Science 281 (1998) 951–956.
[2] H. Ohno, D. Chiba, F. Matsukura, T. Omiya, E. Abe, T. Dietl, Y. Ohno, K. Ohtani, Nature 408 (2000) 944–946.
[3] F. Pan, C. Song, X.J. Liu, Y.C. Yang, F. Zeng, Mater. Sci. Eng. R: Rep. 62 (2008) 1–35.
[4] G. Kunert, S. Dobkowska, T. Li, H. Reuther, C. Kruse, S. Figge, R. Jakiela, A. Bonanni, J. Grenzer, W. Stefanowicz, J.V. Borany, M. Sawicki, T. Dietl, D. Hommel, Appl. Phys. Lett. 101 (2012) 022413.
[5] J. Philip, A. Punnoose, B.I. Kim, K.M. Reddy, S. Layne, J.O. Holmes, B. Satpati, P.R. Leclair, T.S. Santos, J.S. Moodera, Nat. Mater. 5 (2006) 298–304.
[6] N.H. Hong, J. Sakai, W. Prellier, A. Hassini, A. Ruyter, F. Gervais, Phys. Rev. B 70 (2004) 195204.
[7] T. Dietl, Nat. Mater. 9 (2010) 965–974.
[8] S.Q. Zhou, Q.Y. Xu, K. Potzger, G. Talut, R. Grötzschel, J. Fassbender, M. Vinnichenko, J. Grenzer, M. Helm, H. Hochmuth, M. Lorenz, M. Grundmann, H. Schmidt, Appl. Phys. Lett. 93 (2008) 232507.
[9] H. Pan, J.B. Yi, L. Shen, R.Q. Wu, J.H. Yang, J.Y. Lin, Y.P. Feng, J. Ding, L.H. Van, J.H. Yin, Phys. Rev. Lett. 99 (2007) 127201.
[10] R.J. Green, D.W. Boukhvalov, E.Z. Kurmaev, L.D. Finkelstein, H.W. Ho, K.B. Ruan, L. Wang, A. Moewes, Phys. Rev. B 86 (2012) 115212.
[11] C. Zhao, Z. Xu, H. Wang, J.K. Wei, W.L. Wang, X.D. Bai, E.G. Wang, Adv. Funct. Mater. 24 (2014) 5985–5992.
[12] C.F. Yu, S.Y. Chen, S.J. Sun, H. Chou, J. Phys. D: Appl. Phys. 42 (2009) 035001.
[13] S.W. Fan, K.L. Yao, Z.L. Liu, Appl. Phys. Lett. 94 (2009) 152506.
[14] R. Long, N.J. English, Phys. Rev. B 80 (2009) 115212.
[15] H. Pan, Y.P. Feng, Q.Y. Wu, Z.G. Huang, J.Y. Lin, Phys. Rev. B 77 (2008) 125211.
[16] Y.D. Ma, Y. Dai, B.B. Huang, Comput. Mater. Sci. 50 (2011) 1661–1666.
[17] K. Li, X.B. Du, Y. Yan, H.X. Wang, Q. Zhan, H.M. Jin, Phys. Lett. A 374 (2010) 3671–3675.
[18] K.S. Yang, Y. Dai, B.B. Huang, M.H. Whangbo, Appl. Phys. Lett. 93 (2008) 132507.
[19] L. Shen, R.Q. Wu, H. Pan, G.W. Peng, M. Yang, Z.D. Sha, Y.P. Feng, Phys. Rev. B 78 (2008) 073306.
[20] J.G. Tao, L.X. Guan, J.S. Pan, C.H.A. Huan, L. Wang, J.L. Kuo, Z. Zhang, J.W. Chai, S.J. Wang, Appl. Phys. Lett. 95 (2009) 062505.
[21] L.X. Guan, J.G. Tao, C.H.A. Huan, J.L. Kuo, L. Wang, Appl. Phys. Lett. 95 (2009) 012509.
[22] Y.N. Xu, W.Y. Ching, Phys. Rev. B 48 (1993) 4335–4351.
[23] O. Zakharov, A. Rubio, X. Blase, M.L. Cohen, S.G. Louie, Phys. Rev. B 50 (1994) 10780–10787.
[24] H. Murai, T. Abe, J. Matsuda, H. Sato, S. Chiba, Y. Kashiwaba, Appl. Surf. Sci. 244 (2005) 351–354.
[25] Y. Wang, S. Ramanathan, Q. Fan, F. Yun, H. Morkoc, S. Bandyopadhyay, J. Nanosci. Nanotech. 6 (2006) 2077–2080.
[26] M.J. Fernée, A. Watt, J. Warner, S. Cooper, N. Heckenberg, H. Rubinsztein-Dunlop, Nanotechnology 14 (2003) 991–997.
[27] J.P. Perdew, K. Burke, M. Ernzerhof, Phys. Rev. Lett. 77 (1996) 3865–3868.
[28] A. Alkauskas, M.D. Mccluskey, C.G. Van de Walle, J. Appl. Phys. 119 (2016) 181101.
[29] H. Wu, A. Stroppa, S. Sakong, S. Picozzi, M. Scheffler, P. Kratzer, Phys. Rev. Lett. 105 (2010) 267203.
[30] V.I. Anisimov, J. Zaanen, O.K. Andersen, Phys. Rev. B 44 (1991) 943–954.
[31] A. Filippetti, N.A. Spaldin, Phys. Rev. B 67 (2003) 125109.
[32] V. Pardo, W.E. Pickett, Phys. Rev. B 78 (2008) 134427.
[33] A. Droghetti, C.D. Pemmaraju, S. Sanvito, Phys. Rev. B 78 (2008) 140404.
[34] F. Tran, P. Blaha, Phys. Rev. Lett. 102 (2009) 226401.
[35] D.J. Singh, Phys. Rev. B 82 (2010) 205102.
[36] Y. Wang, H.T. Yin, R.G. Cao, F. Zahid, Y. Zhu, L. Liu, J. Wang, H. Guo, Phys. Rev. B 87 (2013) 235203.
[37] A. Manzar, G. Murtaza, R. Khenata, S. Muhammad, Hayatullah, Chin. Phys. Lett. 30 (2013) 067401.
[38] S.D. Guo, B.G. Liu, EPL 93 (2011) 47006.
[39] S.W. Fan, L.J. Ding, Z.L. Wang, K.L. Yao, Appl. Phys. Lett. 102 (2013) 022404.
[40] S.W. Fan, J.H. Dong, L.J. Ding, Z.L. Wang, K.L. Yao, Comput. Mater. Sci. 67 (2013) 83–87.
[41] S.W. Fan, X.P. Huang, L.J. Ding, Z.L. Wang, K.L. Yao, Comput. Mater. Sci. 82 (2014) 345–349.
[42] S.W. Fan, T. Song, K.L. Yao, Comput. Mater. Sci. 106 (2015) 45–49.
[43] S.W. Fan, W.B. Li, X.N. Huang, Z.B. Li, L.Q. Pan, Appl. Phys. Express 8 (2015) 045802.
[44] S.W. Fan, L.J. Ding, K.L. Yao, J. Appl. Phys. 114 (2013) 113905.
[45] Y.H. Zhao, Y.F. Li, Y. Liu, Appl. Phys. Lett. 100 (2012) 092407.
[46] K. Schwarz, P. Blaha, G.K.H. Madsen, Comput. Phys. Commun. 147 (2002) 71–76.
[47] S.J. Clark, M.D. Segall, C.J. Pickard, P.J. Hasnip, I.J. Probert, K. Refson, M.C. Payne, Z. Krist. 220 (2005) 567–570.
[48] S.H. Wei, S.B. Zhang, Phys. Rev. B 62 (2000) 6944–6947.
[49] ⟨http://www.webelements.com⟩.
[50] M. Seike, A.D. Van, T. Fukushima, K. Sato, H. Katayama-Yoshida, Jpn. J. Appl. Phys. 51 (2012) 050201.
[51] A. Zunger, Appl. Phys. Lett. 83 (2003) 57–59.